

See discussions, stats, and author profiles for this publication at: <https://www.researchgate.net/publication/298409641>

Capture and Simulation of Human Motion Lab Report from Experiments

Article · January 2016

CITATIONS

0

READS

514

2 authors:



Franklin Okoli

Ecole Centrale de Nantes

15 PUBLICATIONS 0 CITATIONS

[SEE PROFILE](#)



Deenadayalan .G

Hindustan University

13 PUBLICATIONS 37 CITATIONS

[SEE PROFILE](#)

Some of the authors of this publication are also working on these related projects:



Cable-driven parallel robots, parallel robots, design, modeling, singularity analysis [View project](#)



Fabrication and characterisation of B-H-G fiber with teak wood particles reinforced hybrid composite [View project](#)

Capture and Simulation of Human Motion Lab Report on Human Movement

Author:

Franklin OKOLI
Deenadayalan GANAPATHY

Supervisors:

Sophie SAKKA

January 4, 2016



1 Introduction

In this Lab we carry out the experiments related to the capture and simulation of human motion. This is a study that makes use of certain tools of biomechanics and is still an active research field.

In particular we are also interested to make measurements of the motion of a human body (in this case our actor), make observations from these measurements and make some inference. The measurements are made using an infra red camera to capture the position of the body in space.

In this study, make use of Modified Hanavan model which is a method widely used in Biomechanics and Anatomy in the study of the human body to estimate the mass of the different segments of the human body. The parameters obtained from measuring our actor are to be used to calculate the Dynamics of the model using the Newton-Euler method to obtain the forces, velocity, and accelerations of the body in motion.

The dynamics calculated are then used to rebuild the motion of this body in a simulation to see how natural the captured motion is, we also make use of a force sensor to make comparison of the forces acting on the body.

2 Human Body Segment Estimation

The Hanvan model was first proposed in 1964 and then modified in 1975. This model proposed to subdivide the human body into segments.

The trunk was divided into 3 segments, with each a cylinder, the hand was chosen to be an ellipsoid of revolution

Modified Hanavan anthropometric approximation

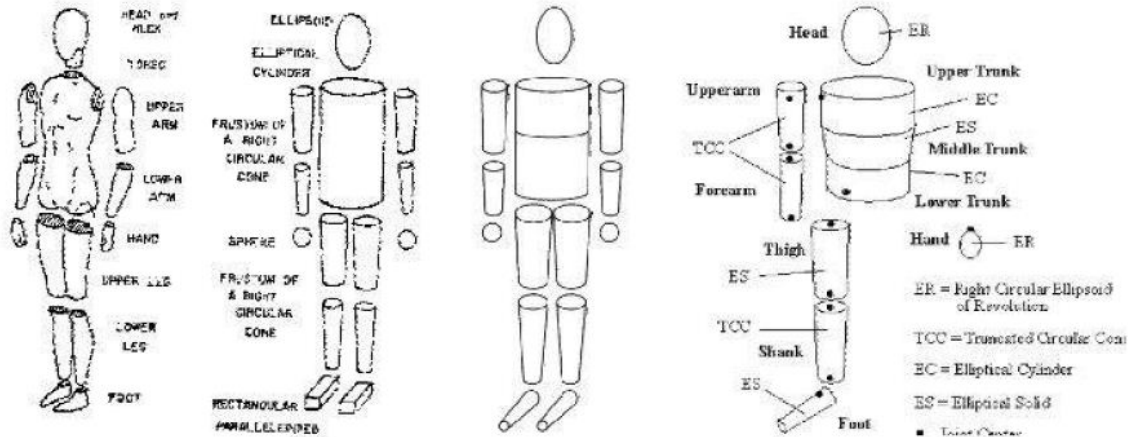


Figure 1: Body Segmentation by Modified Hanavan

and the foot was defined to be an elliptical solid with circular proximal ends. The Thigh was also defined to be an elliptical solid with circular distal ends.

In all, the Modified Hanavan model requires 41 parameters to be measured in the body of the actor. These parameters include:

No	Parameter	No	Parameter
1	L: Hand	21	C: Toe
2	L: Wrist to Knuckle	22	C: Ankle
3	L: Forearm	23	C: Shank
4	L: Upper arm	24	C: Knee
5	L: Elbow to Acromion	25	C: Upper Thigh
6	L: Foot	26	C: Head
7	L: Shank	27	C: Chest
8	L: Thigh	28	C: Xyphion Level
9	L: Head	29	C: Omphalion Level
10	L: Upper Trunk	30	C: Buttock
11	L: Xyphion to Acromion Level	31	W: Hand
12	L: Middle Trunk	32	W: Wrist
13	L: Lower Trunk	33	W: Foot
14	C: Fist	34	W: Toe
15	C: Wrist	35	D: Hip
16	C: Forearm	36	W: Chest
17	C: Elbow	37	W: Xyphion Level
18	C: Axillary Arm	38	W: Omphalion Level
19	C: Foot	39	W: Coxae
20	C: Ball of Foot	40	L: Xyphion Level to Chin/Neck Intersection
41	L: Hip to Chin/Neck Intersection = $P_{12} + P_{13} + P_{40}$		

L: Length; C: Circumference; W: Width; D: Depth



Figure 2: 41 Parameters to be measured on the body of the actor

When we get these parameters, $P_1 \dots P_{41}$ we use them as arguments to BSP functions which help us to estimate the parameters of the geometric shapes that these human body segments have been approximated to. These functions are shown below:

Geometric Shapes and Arguments of the BSP Functions

Segment	Shape	Group	Arguments
Hand	ER	SE	$a = b = \frac{P_{14}}{2\pi}, c = \frac{P_2}{2}$
Forearm	TCC	ES	$a_0 = b_0 = \frac{P_{17}}{2\pi}, a_1 = b_1 = \frac{P_{15}}{2\pi}, L = P_3$
Upperarm	TCC	ES	$a_0 = b_0 = \frac{P_{18}}{2\pi}, a_1 = b_1 = \frac{P_{17}}{2\pi}, L = P_5$
Foot	ES Circ. Base	ES	$a_0 = b_0 = \frac{P_{19}}{2\pi}, a_1 = \frac{P_{33}+P_{24}}{4}, b_1 = \frac{P_{20}+P_{21}}{2\pi}, L = P_6$
Shank	TCC	ES	$a_0 = b_0 = \frac{P_{24}}{2\pi}, a_1 = b_1 = \frac{P_{22}}{2\pi}, L = P_7$
Thigh	ES Circ. Top	ES	$b_0 = \frac{P_{35}}{2}, a_0 = \frac{P_{25}}{\pi} - b_0, a_1 = b_1 = \frac{P_{24}}{2\pi}, L = P_8$
Head	ER	SE	$a = b = \frac{P_{26}}{2\pi}, c = \frac{P_0}{2}$
U Trunk	EC	ES	$a_0 = a_1 = \frac{P_{26}+P_{37}}{4}, b_0 = b_1 = \frac{P_{27}+P_{28}}{2\pi} - a_0, L = P_{11}$
M Trunk	ES	ES	$a_0 = \frac{P_{37}}{2}, a_1 = \frac{P_{38}}{2}, L = P_{12}, b_0 = \frac{P_{28}}{\pi} - a_0, b_1 = \frac{P_{29}}{\pi} - a_1$
L Trunk	EC	ES	$a_0 = a_1 = \frac{P_{38}+P_{39}}{4}, L = P_{13}, b_0 = b_1 = \frac{P_{29}+P_{30}}{2\pi} - a_0$

EC: Elliptical Column, ER: Ellipsoid of Revolution, ES: Elliptical Solid, SE:

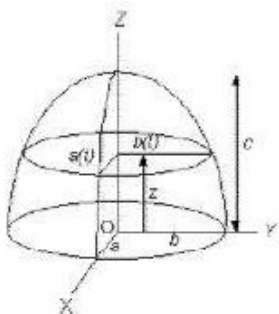
Semi-Ellipsoid, TCC Truncated Circular Cone

146 / 45

Figure 3: Approximation of Human Body segments to Geometric shapes using 41 Modified Hanavan Parameters

Each of these segments that has been approximated to a geometric shape has 5 *Parameters* which are required to calculate its dynamics when it is in motion. These BSP parameters are:

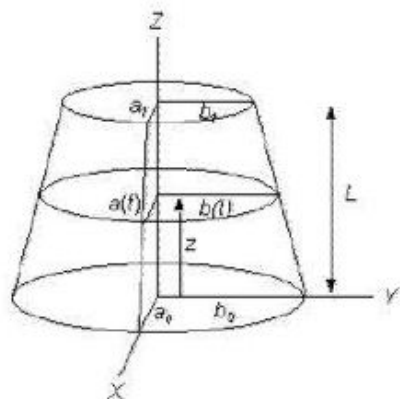
1. Mass
2. Postion of Center of Mass.
3. 3 parameters for the Moment of Inertia I_{xx}, I_{yy}, I_{zz}



Mass	$\frac{2\pi}{3}\rho abc$
CoM pos	$\frac{3}{8}c$
I_{xx}	$\frac{1}{5}m[(b^2 + c^2) - (\frac{3}{8}c)^2]$
I_{yy}	$\frac{1}{5}m[(a^2 + c^2) - (\frac{3}{8}c)^2]$
I_{zz}	$\frac{1}{5}m(a^2 + b^2)$

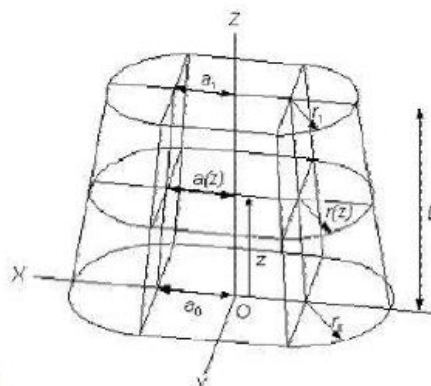
(a) Semi-Ellipsoid group

Elliptical solid (ES)



Mass	$\pi\rho L A_1^{ab}$
CoM pos	$L \frac{A_2^{ab}}{A_1^{ab}}$
I_{xx}	$\frac{1}{4}m \frac{A_4^{bbbb}}{A_1^{ab}} + mL^2 \frac{A_3^{ab}}{A_1^{ab}} - m(L \frac{A_2^{ab}}{A_1^{ab}})^2$
I_{yy}	$\frac{1}{4}m \frac{A_4^{aaaa}}{A_1^{ab}} + mL^2 \frac{A_3^{ab}}{A_1^{ab}} - m(L \frac{A_2^{ab}}{A_1^{ab}})^2$
I_{zz}	$\frac{1}{4}m \frac{A_4^{aaaab} + A_4^{bbbb}}{A_1^{ab}}$

(b) Elliptical Solid group



Stadium solid (SS)

Mass	$\rho L(4A_1^{ar} + \pi A_1^{rr})$
CoM	$L \frac{4A_2^{ar} + \pi A_2^{rr}}{4A_1^{ar} + \pi A_1^{rr}}$
I_{xx}	$\frac{m}{4A_1^{ar} + \pi A_1^{rr}} \left(\frac{4L}{3} A_4^{arrr} + \frac{\pi L}{4} A_4^{rrrr} + 4L^3 A_3^{ar} + \frac{\pi L^3}{2} A_3^{rr} - \frac{(4A_2^{ar} + \pi A_2^{rr})^2}{4A_1^{ar} + \pi A_1^{rr}} \right)$
I_{yy}	$\frac{m}{4A_1^{ar} + \pi A_1^{rr}} \left(\frac{4L}{3} A_4^{aaar} + \pi L A_4^{aarr} + \frac{8L}{3} A_4^{arrr} + \frac{\pi L}{4} A_4^{rrrr} + 4L^3 A_3^{ar} + \frac{\pi L^3}{2} A_3^{rr} - \frac{(4A_2^{ar} + \pi A_2^{rr})^2}{4A_1^{ar} + \pi A_1^{rr}} \right)$
I_{zz}	$\frac{mL}{4A_1^{ar} + \pi A_1^{rr}} \left(\frac{4}{3} A_4^{aaar} + \pi A_4^{aarr} + 4A_4^{arrr} + \frac{\pi}{2} A_4^{rrrr} \right)$

(c) State Solid group

Figure 1: Different geometric groups used in the Modified Hanavan model

2.1 Measurements

We carried out experiments where each group measured the actor independently to obtain the 41 parameters and we see the results from the measurement below:

	A	B	C	D	E	F	G	H	I
1	No	eBona_Manca	Labolani_Lottero_Olivi	Franklin_Deena	Rasheed_Caterin	Mean	Standard Deviation	Mean_in_meters	
2	1	19.1	20.3	20.5	18	19.1	1.019803903	0.194	
3	2	9	9.4	11	10.5	10.1	0.809320703	0.1	
4	3	27.2	25.1	29	32	28.5	2.532390175	0.2836	
5	4	35	31.5	33	33	32.1	1.325518766	0.3292	
6	5	37.4	35.8	33.5	32	35.5	2.107842499	0.3484	
7	6	27	27	27	27.5	26.4	2.389871774	0.2698	
8	7	32	40.3	38	43	40.3	3.106308214	0.3992	
9	8	38	42.2	41	44.5	39.6	5.784289066	0.3906	
10	9	19.5	22.6	23.5	22.4	21.8	1.504327092	0.2196	
11	10	20	20.7	22	17.5	23.1	2.186	4.366119559	0.2186
12	11	29	28.6	32	18	22	5.738640954	0.2592	
13	12	8	8.3	8	30.5	9	12.76	9.92537153	0.1276
14	13	16	17.6	20	13.5	14.8	2.526262061	0.1638	
15	14	28.4	27.3	27.5	29.4	28.3	2.818	0.834865259	0.2818
16	15	17.6	17.2	19	17	17	0.841427359	0.1756	
17	16	24.4	26.4	23.5	27.1	26.7	2.562	1.577022511	0.2562
18	17	25.5	26.3	25.5	27	26.2	0.628490254	0.261	
19	18	32	30.9	33	31.3	30.95	3.163	0.882892972	0.3163
20	19	22.3	25.2	26	23	24.7	2.424	1.543696861	0.2424
21	20	23.8	25.5	26.5	18.5	21.45	2.315	3.228002478	0.2315
22	21	8	8.6	9	8	8.1	0.834	0.444971909	0.0834
23	22	22.3	23.3	23.5	26.8	27.4	2.466	2.283199509	0.2466
24	23	38	28.9	37.5	35.7	34.5	3.492	3.645819524	0.3492
25	24	36	38	46	38	36.5	3.89	4.068163121	0.389
26	25	44	48	35.5	53.2	53.1	46.76	7.375838935	0.4676
27	26	58	58	59	61.5	39.1	55.12	9.089013177	0.5512
28	27	98	99.2	100	96.8	96.9	98.18	1.407835218	0.9818
29	28	86	88.5	87.5	98.5	86.9	89.48	5.123670559	0.8948
30	29	76.7	81	77.2	80.7	83.2	79.76	2.746452257	0.7976
31	20	94	93.8	93.5	96.5	93.3	94.22	1.302689526	0.9422
32	31	9.4	10.6	9.8	10.4	11.7	10.38	0.878635305	0.1038
33	32	6.4	6.7	6.8	8.8	6.3	7	1.027131929	0.07
34	33	9	7.8	9	11	10.3	9.42	1.249739984	0.0942
35	34	2.5	3.4	3	2.9	2.3	2.82	0.432434966	0.0282
36	35	15	17.7	16	21.5	21.5	18.34	3.041874422	0.1834
37	36	33	32	32.5	35.5	30.1	32.62	1.948589233	0.3262
38	37	29	29.5	28.9	33.8	28.6	29.96	2.170944495	0.2996
39	38	29.5	29.3	30	35.5	31.8	31.22	2.587856256	0.3122
40	29	30	31.5	31	33.5	27.5	30.7	2.196588264	0.307
41	20	27	31.5	29	28.5	34.6	30.12	2.982783935	0.3012
42	41	51	57.4	57	65.5		57.725	5.952800461	0.57725

Figure 4: Hanavan Measurements from the 5 Groups

From these measurements, we see that each group generates quite different values for the same parameter and the same Actor. This shows that the accuracy of this technique and reproducibility of the results can be affected by the method used for taking the measurement. Below we show a sample image of how we measure the Length, width and circumference of the arm of our Actor.



Figure 5: Measuring the Arm of our Actor

Other groups have obtained different results from making the same measurement and we can compare the results by looking at the mean and standard deviation of some measurements.

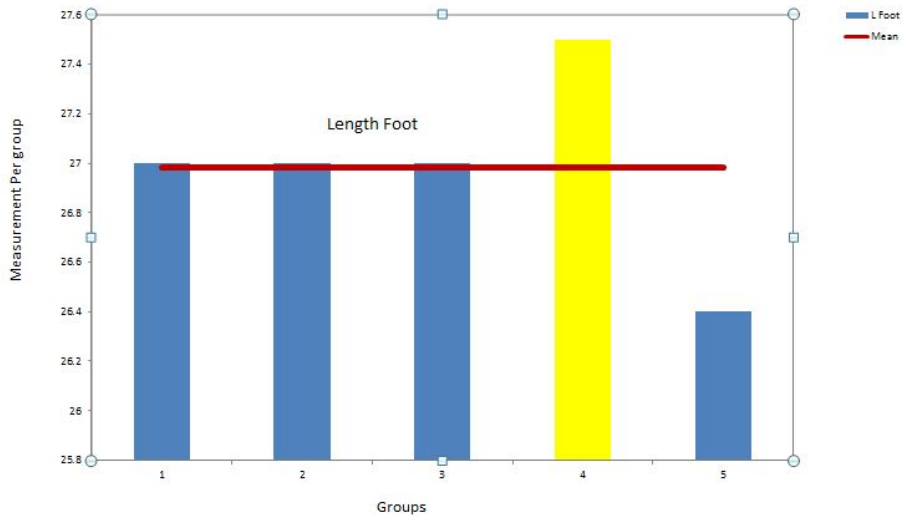


Figure 6: Comparing the measurements of the Length of foot

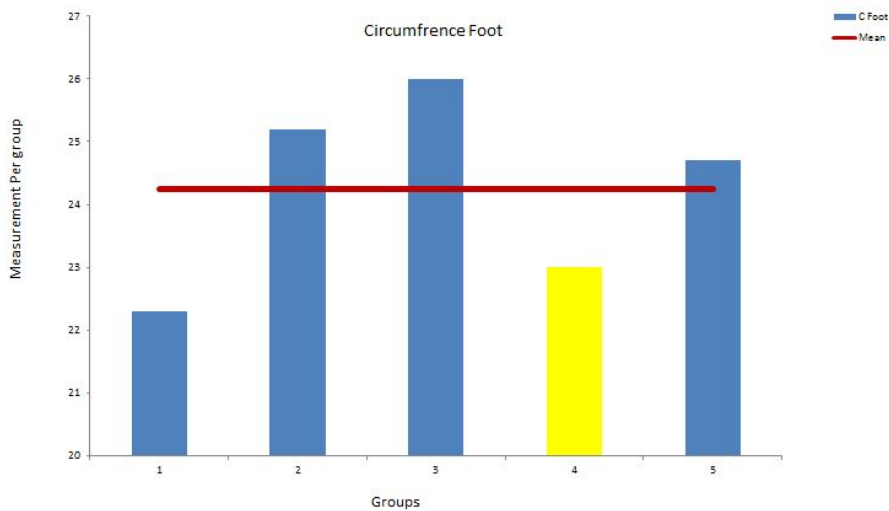


Figure 7: Comparing the measurements of the Circumference of foot

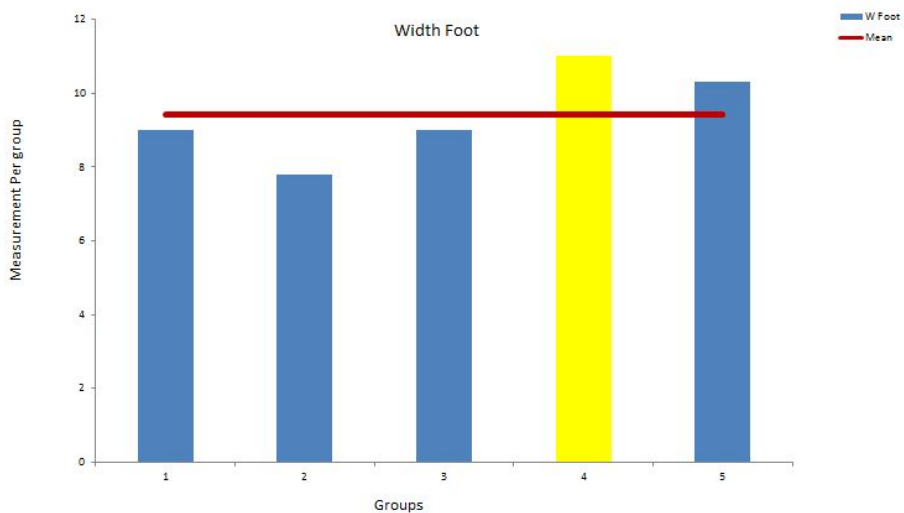


Figure 8: Comparing the measurements of the width of foot

From the above, we see that different groups come up with different measurement value for the same actor on the same parameter. This is a classical problem in Biomechanics and we can further see this from the plot of the standard deviation:

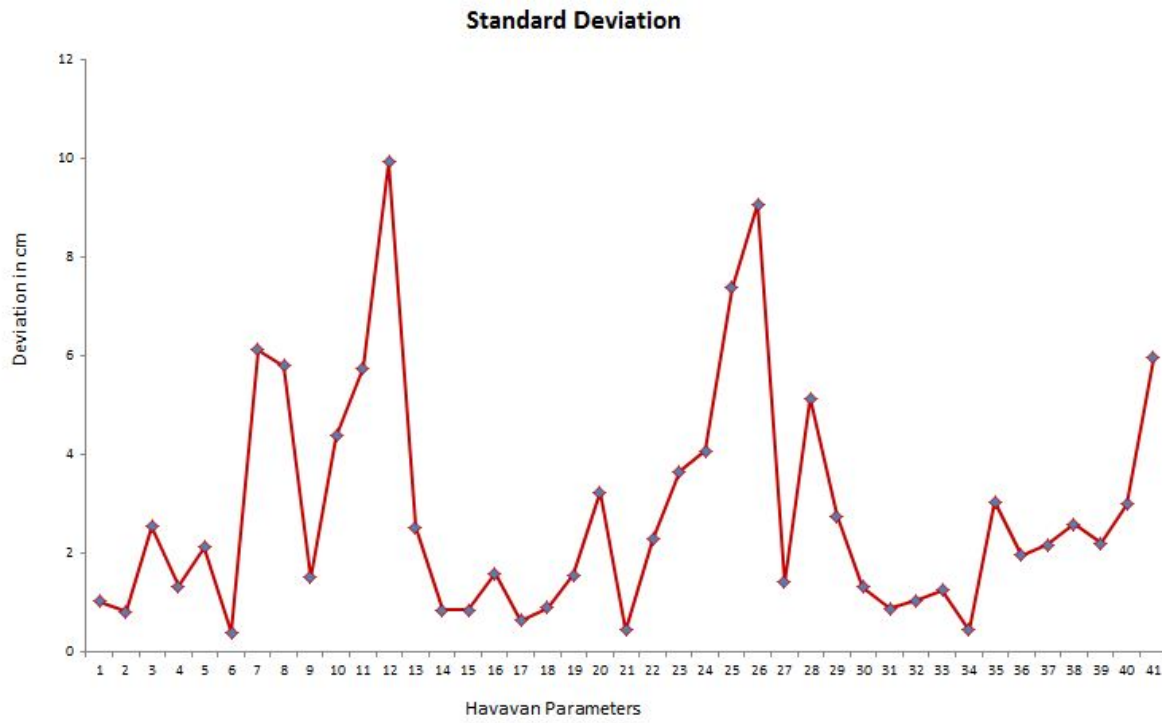


Figure 9: Standard deviation observed for all 41 Parameters

From the above, we cannot say that the measurement of any of the 5 groups is the best or can accurately fit the actual size of the actor. As a matter of compromise, we propose to use the mean values for each of the parameters to carry out the experiments.

3 Programming

In this section, we implement basic models of the Newton-Euler Algorithm as applied to an inverted single pendulum and a double inverted pendulum.

3.1 Modelling the Inverted Single Pendulum

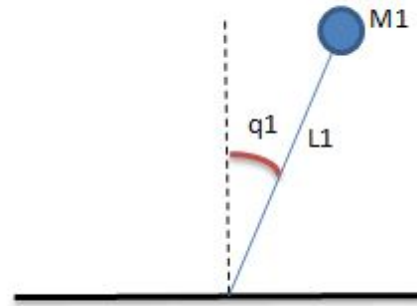


Figure 10: The Inverted Single Pendulum

The equations for the Kinematics and dynamics for this link are given below as:

Position:

$$x_1 = -l_1 \sin(q_1) \quad (1)$$

$$y_1 = l_1 \cos(q_1) \quad (2)$$

Velocity:

$$\dot{x}_1 = -l_1 \cos(q_1) \dot{q}_1 \quad (3)$$

$$\dot{y}_1 = -l_1 \sin(q_1) \dot{q}_1 \quad (4)$$

Acceleration:

$$\ddot{x}_1 = l_1 \sin(q_1) \dot{q}_1^2 - l_1 \cos(q_1) \ddot{q}_1 \quad (5)$$

$$\ddot{y}_1 = -l_1 \cos(q_1) \dot{q}_1^2 - l_1 \sin(q_1) \ddot{q}_1 \quad (6)$$

Forces and Torques:

$$m_1 \ddot{x}_1 = F_{x1} \quad (7)$$

$$m \ddot{y}_1 = F_{y1} - m_1 g \quad (8)$$

where F_{x1} and F_{y1} represent the reaction forces on the link from the fixed point.

$$\tau_1 = m_1 l_1^2 \ddot{q}_1 + m_1 g l_1 \sin(q_1) \quad (9)$$

From these models, we plot the motion of the single link under simulation, its velocity, acceleration and the reaction forces. We obtain the plot shown below:

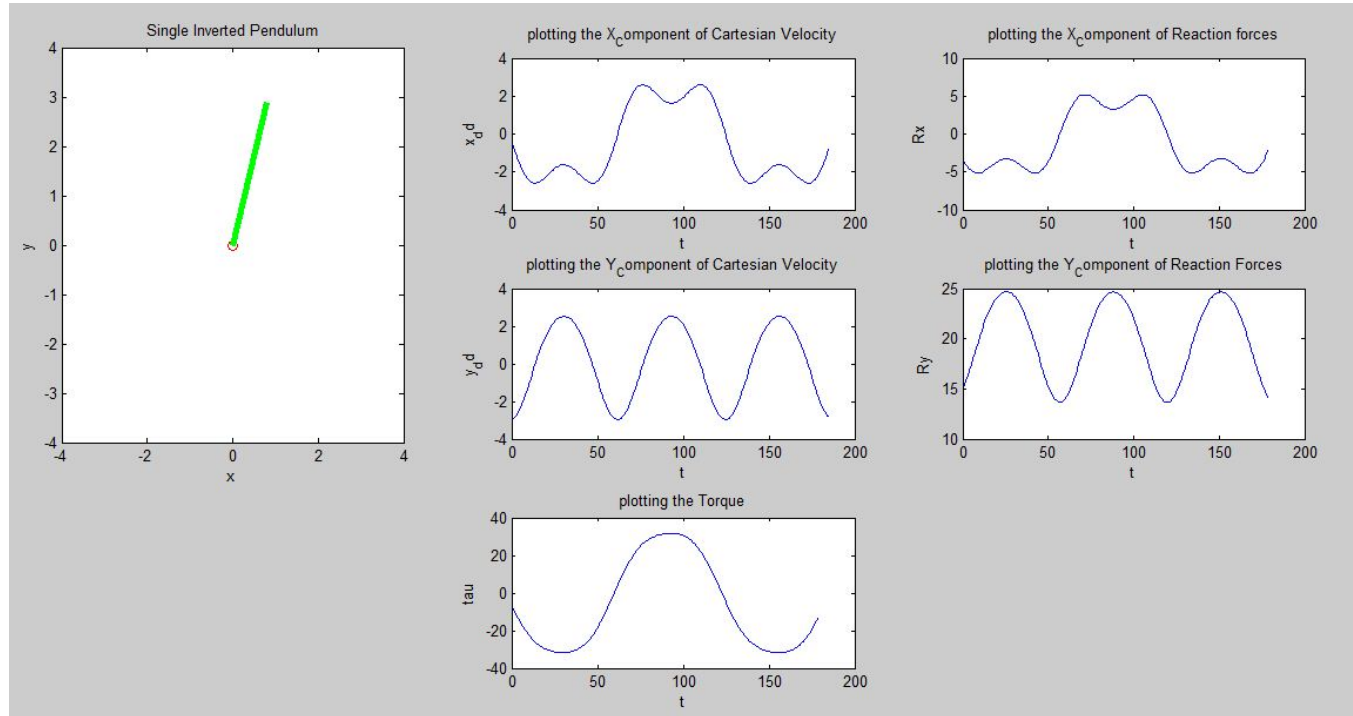


Figure 11: Plots for the Inverted single pendulum

3.2 Modelling the Inverted Double Pendulum

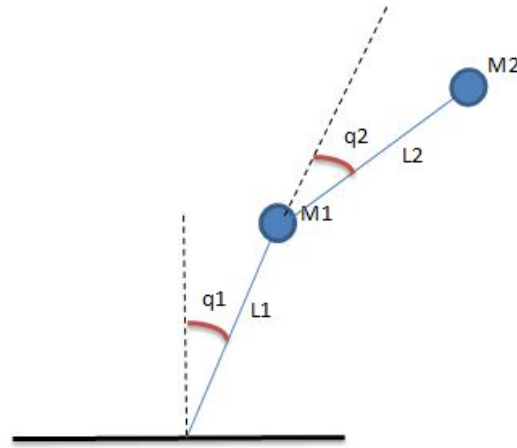


Figure 12: The Inverted Double Pendulum

The equations for the Kinematics and dynamics for these links are given below as:

Position:

$$x_1 = -l_1 \sin(q_1) \quad (10)$$

$$y_1 = l_1 \cos(q_1) \quad (11)$$

$$x_2 = -l_1 \sin(q_1) - l_2 \sin(q_1 + q_2) \quad (12)$$

$$y_2 = l_1 \cos(q_1) + l_2 \cos(q_1 + q_2) \quad (13)$$

Velocity:

$$\dot{x}_1 = -l_1 \cos(q_1) \dot{q}_1 \quad (14)$$

$$\dot{y}_1 = -l_1 \sin(q_1) \dot{q}_1 \quad (15)$$

$$\dot{x}_2 = -l_1 \cos(q_1) \dot{q}_1 - l_2 \cos(q_1 + q_2) (\dot{q}_1 + \dot{q}_2) \quad (16)$$

$$\dot{y}_2 = -l_1 \sin(q_1) \dot{q}_1 - l_2 \sin(q_1 + q_2) (\dot{q}_1 + \dot{q}_2) \quad (17)$$

Acceleration:

$$\ddot{x}_1 = l_1 \sin(q_1) \dot{q}_1^2 - l_1 \cos(q_1) \ddot{q}_1 \quad (18)$$

$$\ddot{y}_1 = -l_1 \cos(q_1) \dot{q}_1^2 - l_1 \sin(q_1) \ddot{q}_1 \quad (19)$$

$$\ddot{x}_2 = -l_1 \cos(q_1) \ddot{q}_1 + l_1 \sin(q_1) \dot{q}_1^2 - l_2 \cos(q_1 + q_2) (\ddot{q}_1 + \ddot{q}_2) + l_2 \sin(q_1 + q_2) (\dot{q}_1 + \dot{q}_2)^2 \quad (20)$$

$$\ddot{y}_2 = -l_1 \sin(q_1) \ddot{q}_1 + l_1 \sin(q_1) \dot{q}_1^2 - l_2 \sin(q_1 + q_2) (\ddot{q}_1 + \ddot{q}_2) + l_2 \cos(q_1 + q_2) (\dot{q}_1 + \dot{q}_2)^2 \quad (21)$$

Forces and Torques:

$$m_1 \ddot{x}_1 = F_{x1} + F_{x2} \quad (22)$$

$$m_1 \ddot{y}_1 = F_{y1} + F_{y2} - m_1 g \quad (23)$$

$$m_2 \ddot{x}_2 = F_{x2} \quad (24)$$

$$m_2 \ddot{y}_2 = F_{y2} - m_2 g \quad (25)$$

where F_{x1}, F_{x2}, F_{x3} and F_{y1}, F_{y2}, F_{y3} represent the reaction forces on the link from the fixed point.

$$\tau_1 = m_1 l_1^2 \ddot{q}_1 + m_1 g l_1 \sin(q_1) \quad (26)$$

$$\tau_2 = m_2 l_2^2 (\ddot{q}_1 + \ddot{q}_2) + m_2 g l_2 \sin(q_1 + q_2) \quad (27)$$

From these models, we plot the motion of the double link under simulation, its velocity, acceleration and the reaction forces. We obtain the plot shown below:

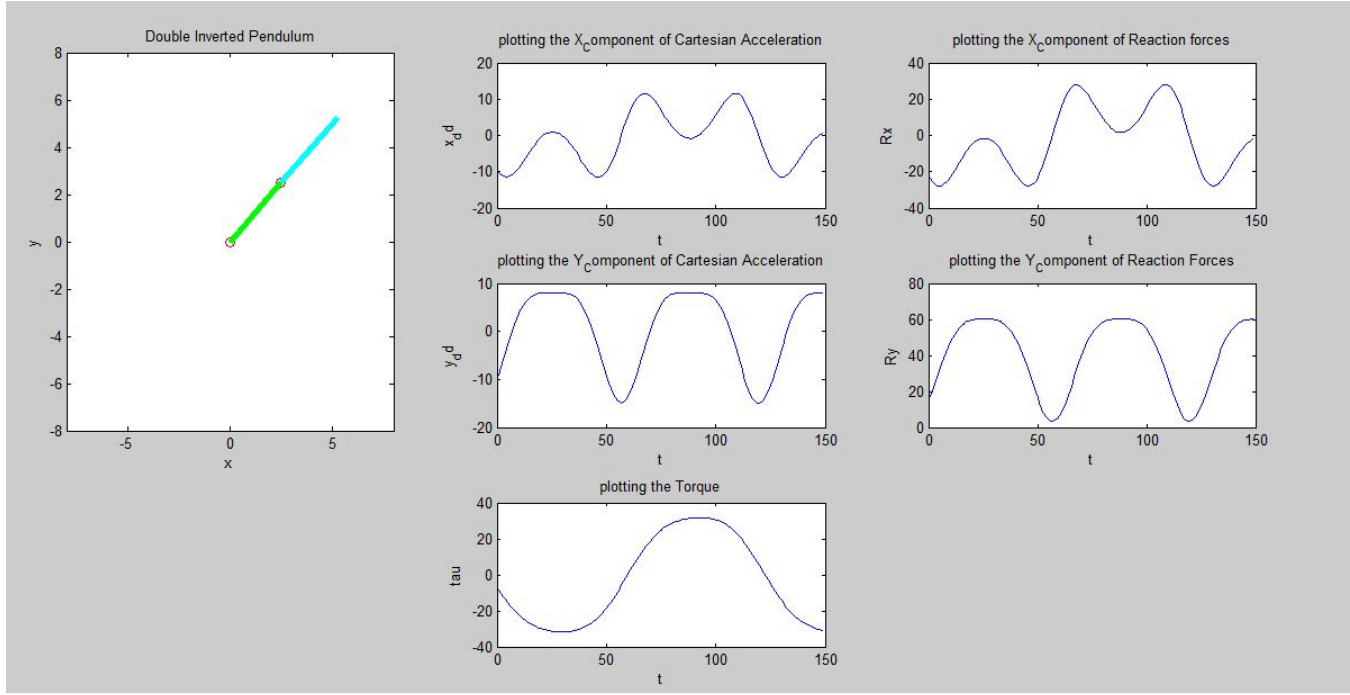


Figure 13: Plots for the Inverted Double pendulum

4 Working Hypothesis

We have made two hypothesis to help us in this experiment:

1. Hypothesis 1: The system is Rigid: This Hypothesis assumes that the human body segments are rigid and therefore we can apply the Newton-Euler equations (which are equations of rigid body to them). But in reality the outermost body of the human which is the skin on which the motion capture devices are affixed are not rigid and are flexible in nature.
2. Hypothesis 2: The moving Body is made of Homogeneous Material:
This is particularly important where we use the predictive equations to estimate the mass of the segments by an integration of a point mass over a volume. This property does not correspond to the real human body where the mass distribution is different depending on the segment being considered.
3. Hypothesis 3 : The system is Energy Conservative: This says that the sum of the Kinetic Energy and Potential Energy at all times is a constant which means that there is no loss or gain of energy from the environment.

4.1 Experimental Protocol

- *Objective:* The objective of this experiment is to capture, simulate and analyze human motion in order to see how closely we can reproduce this motion.

- *The studied Motion:* During this experiment, we have studied 5 kinds of motions that could be possibly performed by a human. They include: waving, kicking, jumping and sitting. Each of these motions are performed by an actor at different speeds, i.e. slow, medium, fast.
- *The Studied Population:* The subject is a Male, 1.88m in height and 80kg in weight. We note here that the study of a single subject cannot be said to constitute a population. A population contains a minimum of 10 subjects according to ISB standards, however, we have made this study as a way of learning the methodology and for educational purpose.
- *Measurement Devices:* The measurement of the motion of the actor is done in a closed room equipped with *ARTtrack* system. This room is cube shaped and contains 8 infra-red cameras which are positioned on the 4 upper and 4 lower vertices of a cube-shaped room. The subject is equipped with measurement markers in each of his body segments, 15 markers since we are using modified-hanavan method. Each Infra-red cameras is able to detect body markers which have been worn by the actor and calculate the 6 – *DOF* position and orientation. The data collected during this camera measurement is stored in a *.drf* file for further processing. We use another measurement device which is a force plate to measure the forces from the actor on the ground, this force values are used to compare to the value obtained from the Newton-Euler computation of forces to see how closely we have estimated the measurements (Experimental Control).

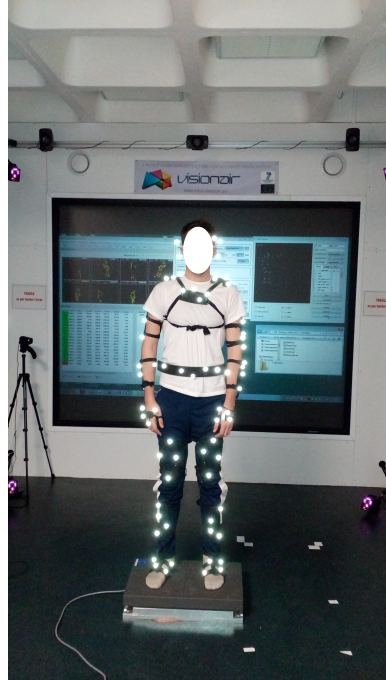


Figure 14: The Actor equipped with Markers and standing on a Force Plate



Figure 15: The Infra-red Camera in one vertex of the Room

We note that the *ARTtrack* system requires to be calibrated before the use of the system to capture motion. This is important to re-initialize the infra-red cameras to ensure that all cameras are able to see all 4 points on a marker. Also if it happens that after calibration, there is a slight push or change in the position of any of the cameras, the entire system needs to be re-calibrated.

We also note that the data capture system is limited by its buffer size, since the camera gives a lot of information per second, therefore it was important for us to only open the system to capture when ready.

- : *Models used:*

The segmentation of the human body was carried out using the modified-Hanavan model. Thus we have 15 body segments where we have fixed the markers during motion to capture their motion data. We made 41 anthropometric measurements of the actor as required by the modified-Hanavan.

These measurements were used to estimate the 5 BSP parameters using the predictive equations for each of the 15 body segments. When we obtain the BSP parameters, they form inputs to be used for the calculation of the forces and moments.

The forces and moments are calculated using newton-Euler formulation. We clearly explain to the Actor that we want to capture his motion while he is making certain gestures, e.g Jumping, kicking, waving.

Then we open the capture system to capture the pose of all his body segments in space at every time instant. This data is saved to a *.drf* file.

In Matlab, we use the provided code *@openfile* to extract the pose at each time instant of a particular motion that was done by the actor and then save this to a multidimensional matrix of size $4 \times 4 \times n$ to a *.mat* file. where n is the number of instants

Then these poses are used in *Animateenergies* to calculate the dynamics by Newton-Euler formulation and plot the resulting Acceleration, Velocity, Position, Energy and forces in all the segments.

The *GenerateBodyHandler* file uses the 41 Modified Hanavan parameters to create the geometric shapes of the segments in order to recreate the entire shape of the Actor in simulation to which we apply the captured motion to see how this movement closely follows real human motion.

- *Methods:*

Some statistical methods used for the comparison of the measured 41 anthropometric parameters of different groups are the mean and the standard deviation.

The mean is defined as:

$$\hat{x} = \frac{1}{N} \sum_{t=1}^N x_t \quad (28)$$

while the standard deviation is defined as:

$$\sigma = \sqrt{\frac{1}{N-1} \sum_{t=1}^N (x_t - \hat{x})^2} \quad (29)$$

We make the numerical derivation to obtain the velocity and acceleration of each body segment from its measured position by using the second order central finite differences.

5 Simulation Results

5.1 Motion 1: Waving Arms

In this motion, we ask the actor to have his arms at three different speeds; slow, medium and fast. Below, we see the plots of the motion: *SlowWave*

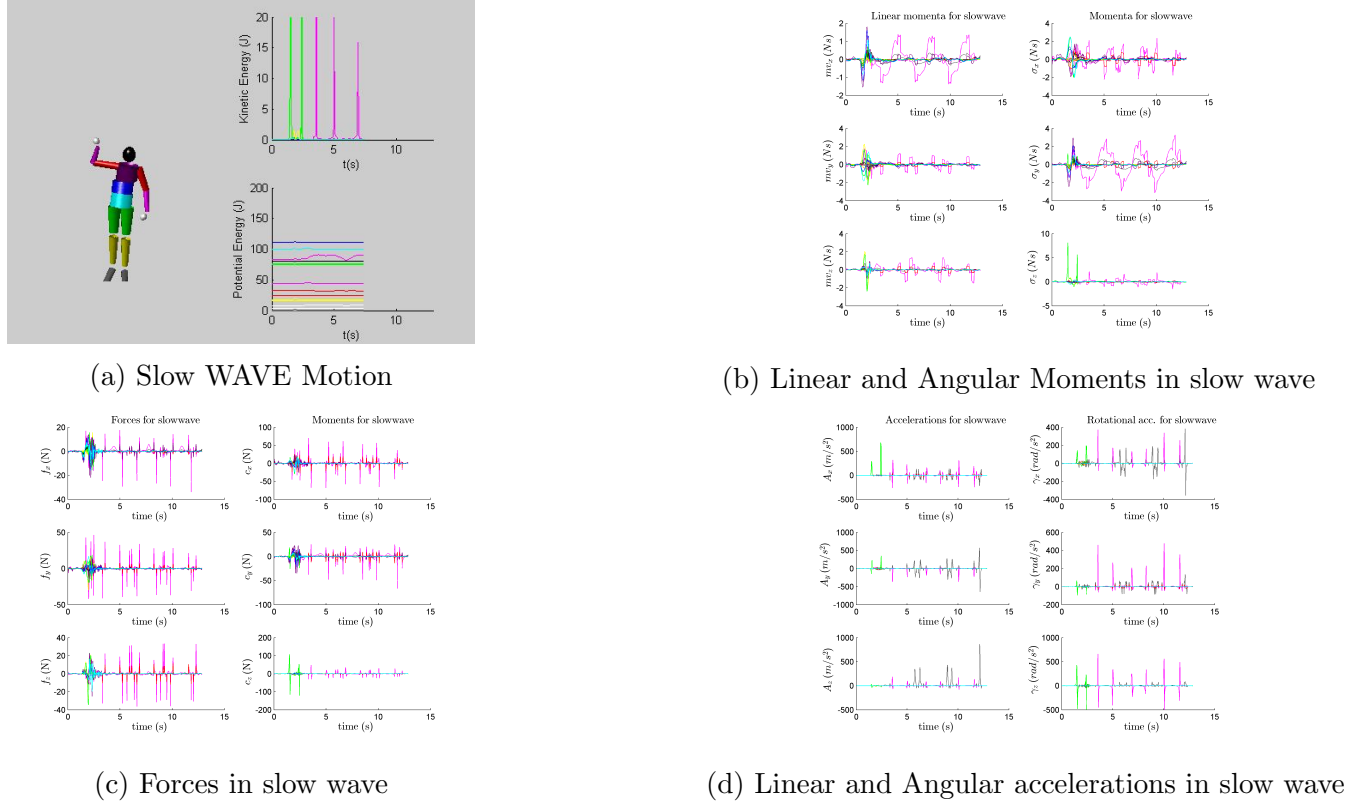
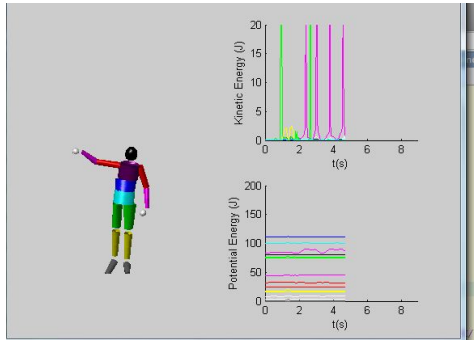


Figure 16: Plots for slow waving

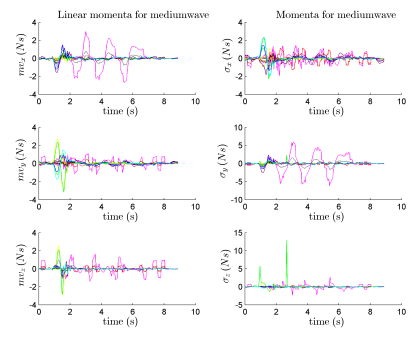
Above we see in the kinetic energy plot the purple spikes corresponding to the arm segment when it is waving. The initial green spike in kinetic energy occurs because we have asked the actor to raise the right leg before waving. We also see in the potential energy plot that the purple undulation corresponds to the motion of the arm during waving

This same is seen in the plots for the forces and moments, we see that the highest values corresponding to the segment in motion which is the arm is seen in the plots in purple colour.

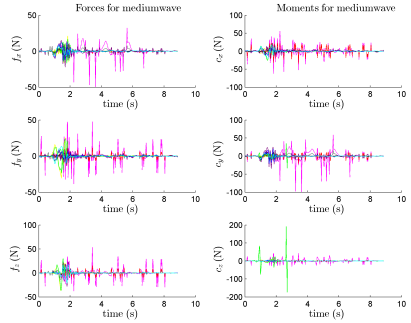
We see similar plots in the plots for medium and fast motion



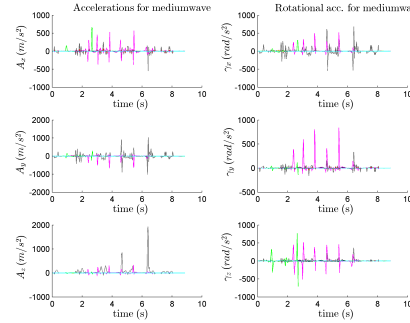
(a) Medium WAVE Motion



(b) Linear and Angular Moments in medium wave

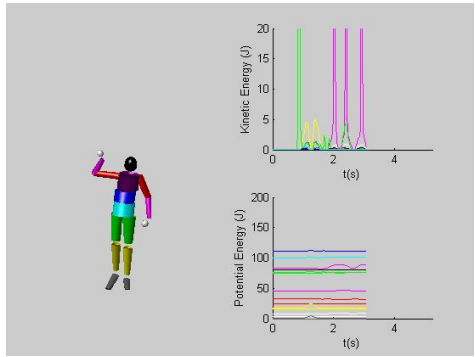


(c) Forces in medium wave

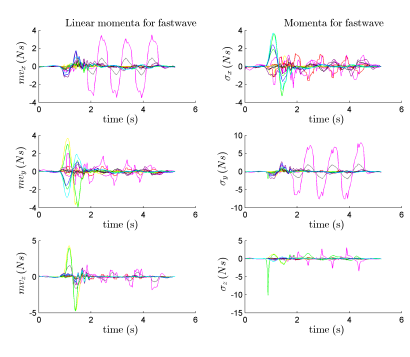


(d) Linear and Angular accelerations in medium wave

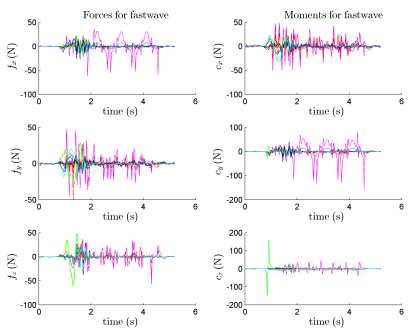
Figure 17: Plots for medium waving



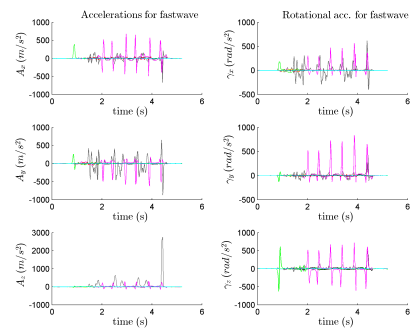
(a) fast wave motion



(b) Linear and Angular Moments in fast wave



(c) Forces in fast wave

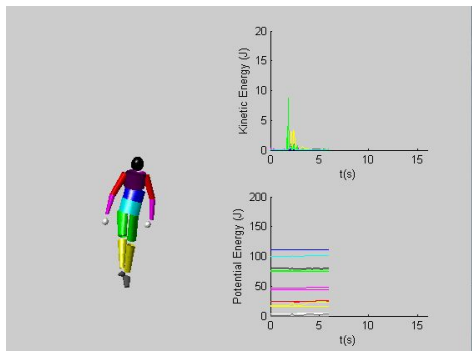


(d) Linear and Angular accelerations in fast wave

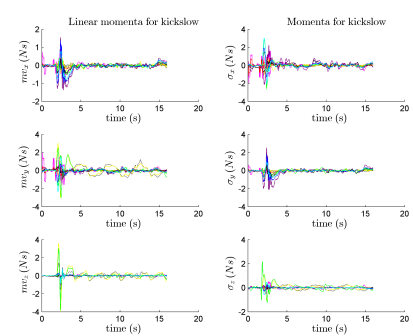
Figure 18: Plots for fast waving

5.2 Motion 2: Kicking with the legs

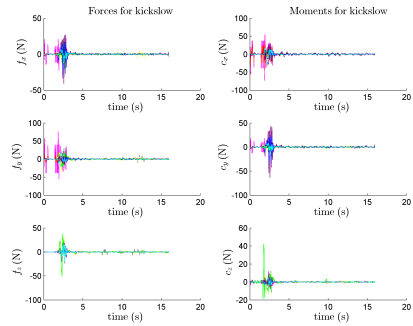
In this motion, we ask the actor to kick with his legs at three different speeds; slow, medium and fast. Below, we see the plots of the motion:



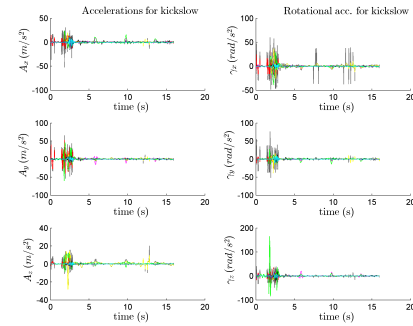
(a) Slow kick Motion



(b) Linear and Angular Moments in slow kick

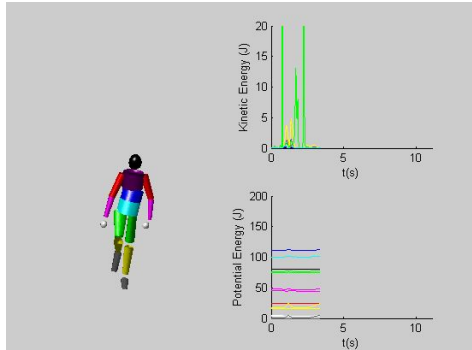


(c) Forces in slow kick

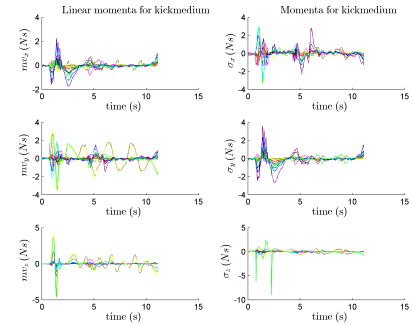


(d) Linear and Angular accelerations in slow kick

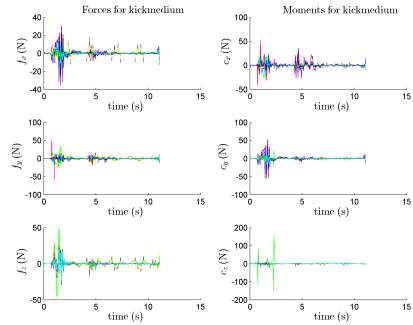
Figure 19: Plots for slow kick



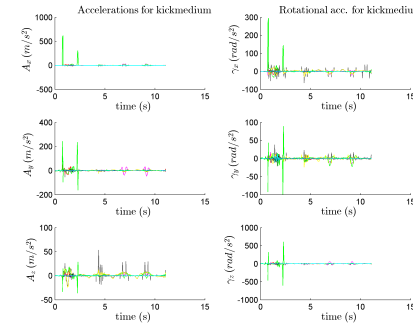
(a) medium kick Motion



(b) Linear and Angular Moments in medium kick

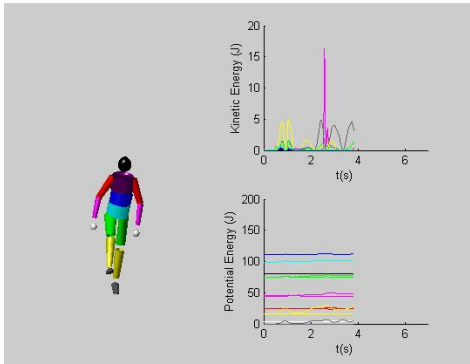


(c) Forces in medium kick

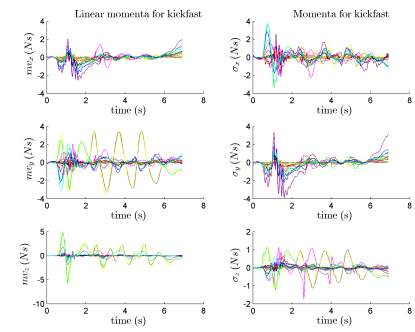


(d) Linear and Angular accelerations in medium kick

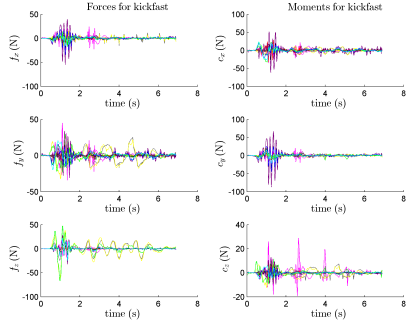
Figure 20: Plots for medium kick



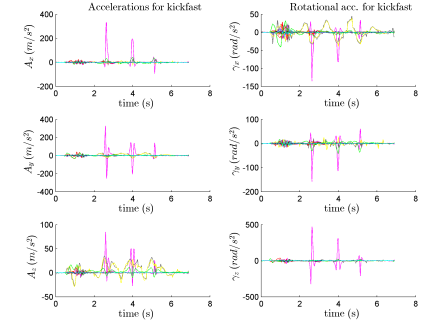
(a) fast kick Motion



(b) Linear and Angular Moments in fast kick



(c) Forces in fast kick



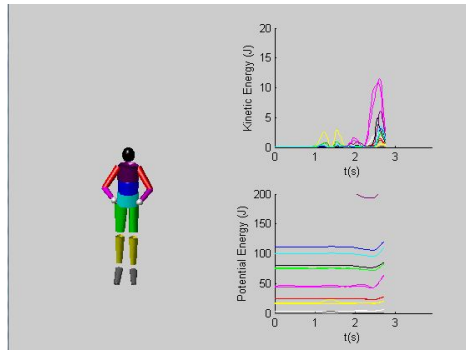
(d) Linear and Angular accelerations in fast kick

Figure 21: Plots for fast kick

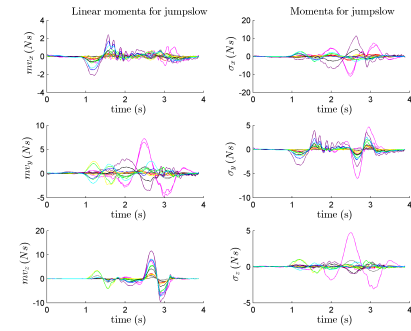
Above we see in the kinetic energy plot the green and yellow spikes corresponding to the right leg upper and lower segment when it is kicking. The amplitude of this spike in kinetic energy is a good indicator that this kick is a slow motion. This can be seen when we compare this to the medium and fast kicking as shown. There is more amplitude when we are kicking faster in the kinetic energy plot. Another thing we notice is that when we try to kick faster, the actor uses his arms to balance the body so we start to see the purple segment moving with higher kinetic energy in the fast kick sequence.

5.3 Motion 3: Jump Motion

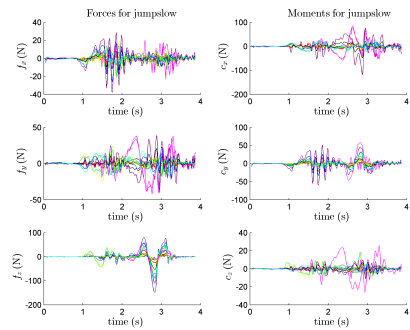
In this motion, we ask the actor to Jump at three different speeds; slow, medium and fast. Below, we see the plots of the motion:



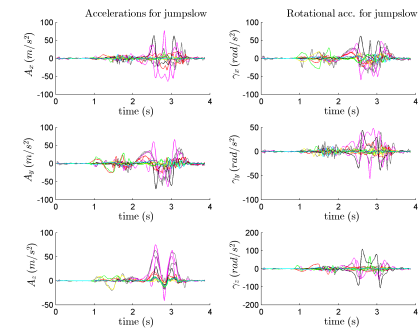
(a) Slow Jump Motion



(b) Linear and Angular Moments in slow Jump

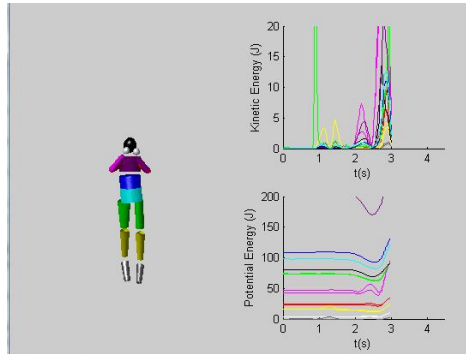


(c) Forces in slow Jump

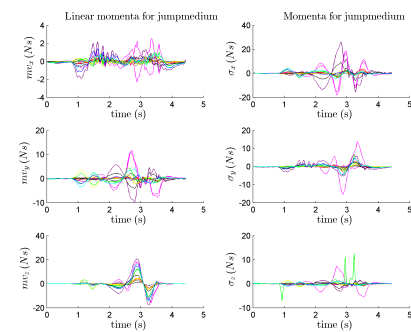


(d) Linear and Angular accelerations in slow Jump

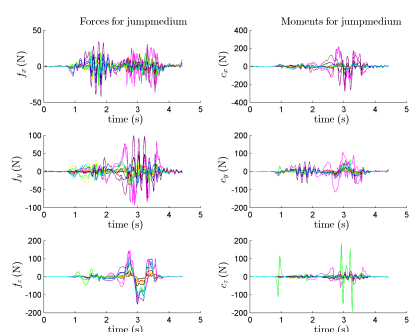
Figure 22: Plots for slow Jump



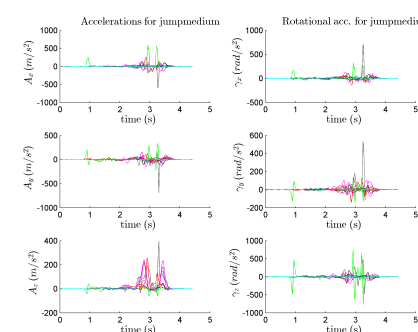
(a) Medium Jump Motion



(b) Linear and Angular Moments in Medium Jump

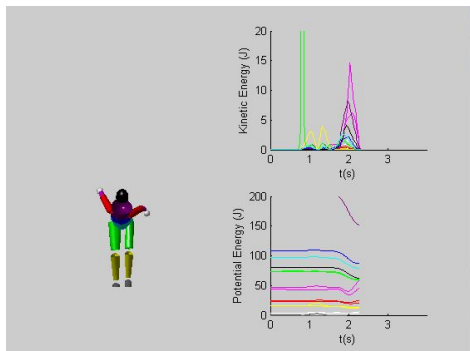


(c) Forces in Medium Jump

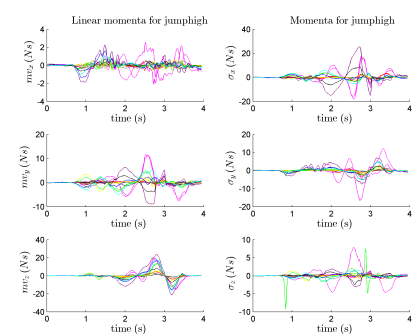


(d) Linear and Angular accelerations in Medium Jump

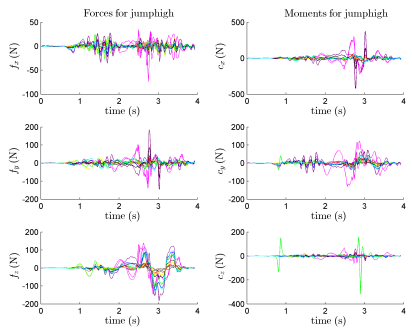
Figure 23: Plots for Medium Jump



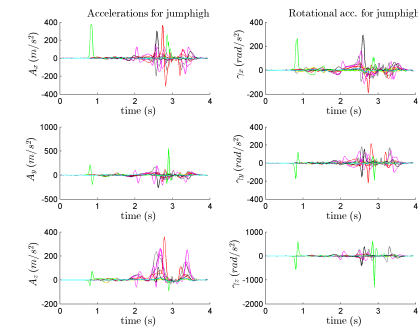
(a) Fast Jump Motion



(b) Linear and Angular Moments in Fast Jump



(c) Forces in Fast Jump



(d) Linear and Angular accelerations in Fast Jump

Figure 24: Plots for Fast Jump

5.4 Motion 4: sit Motion

In this motion, we ask the actor to sit, and then we plot the parameters of this motion. From here we see that the motion closely resembles the natural ghuman sitting. This is seen below:

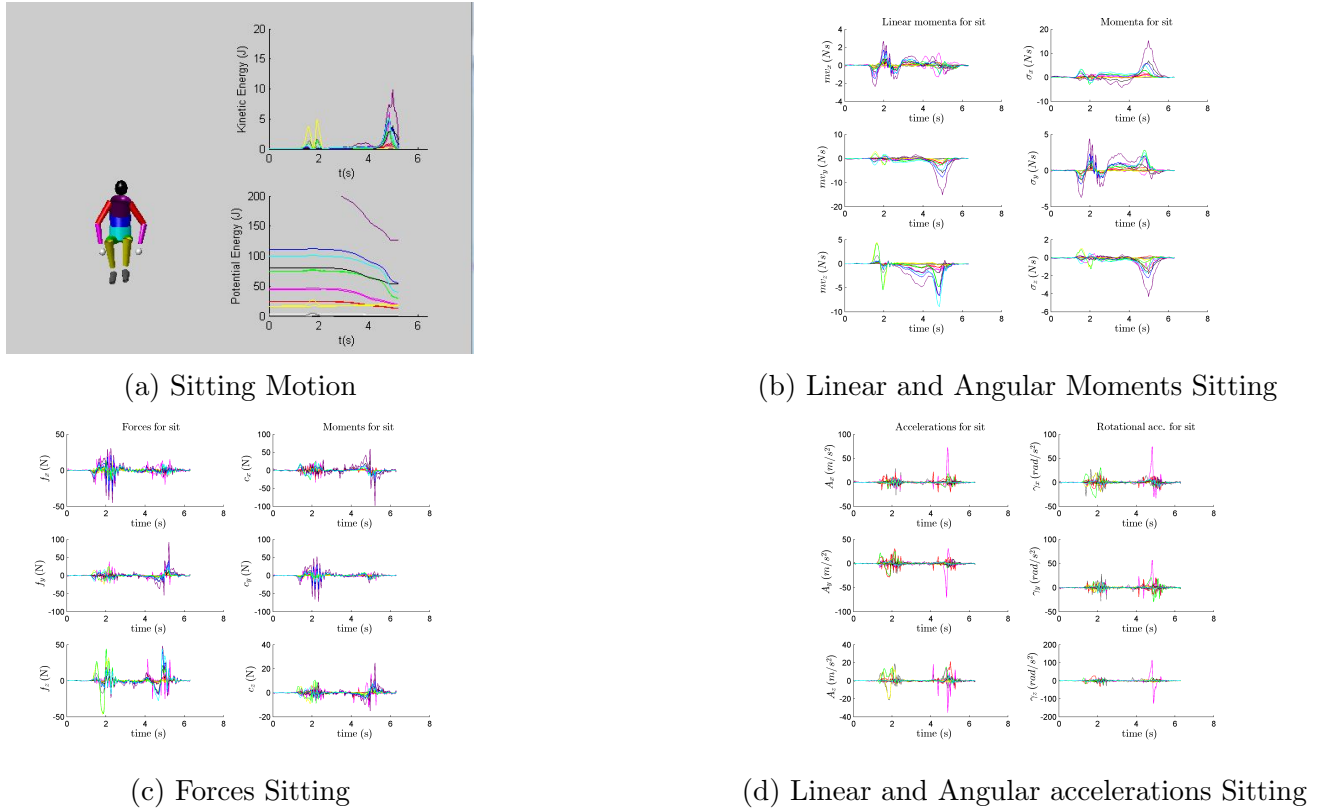


Figure 25: Plots for Sitting

6 Synthesis

As a conclusion we list here in the following some of our main remarks regarding the overall execution of the experiment and we also answer to some of the questions of the assignment:

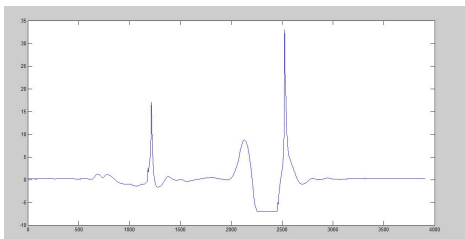
Difficulties during the experiment

The difficulties we faced during the experiments are: We had to choose the correct reading to use for the experiment from the readings of 5 different groups which were all very different for the 41 measurements. We overcame this problem by choosing the mean values.

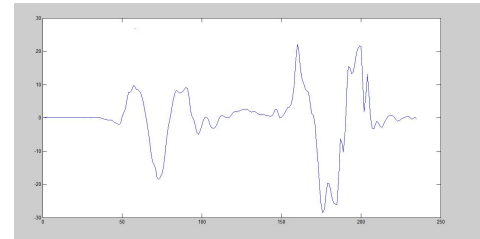
While capturing motions we had to look carefully to see whether the motion capture system loses track of a marker on the actor. If this happens then the data is not recorded.

We faced big difficulty when saving the captured motions in *.drf* format after saving when we start our next motion capture experiment we were not able to save due to the maintenance being carried out on the same intermittently affecting the software. After we must restart our process from beginning to rectify this problem. The software of the *ARTTrack* motion caption system has a limited buffer size which means that the buffer gets filled up very quickly and caused the program to crash. We overcame this problem by only starting the capture when we require the actor to perform a motion otherwise the buffer is closed at all other times.

Propose a conclusion comparing the reaction forces obtained by the mathematical model and the measurements obtained by the force plate
 We can notice the same evolution of the ground reaction forces and of the forces predicted by our model up to some scaling factor. We can see a comparison in the fast jump motion below:



(a) Forces Measured from the force plate



(b) Forces calculated from the Newton Euler for the same motion

- Here we extract the forces in the last segment during this motion that is in contact with the environment and compare it with the forces measured on the force plate during this same motion.
- We see that its difficult to make an accurate comparison of both forces since the force plate generates about 4000 samples for the same motion that the newton-Euler calculated forces obtained using the infra red camera generates about 250 samples. This is seen in the figure above
- Never the less, we see quite a similar shape in the forces acting at this body segment with the peaks at impact and valleys when the body is freely suspended in the air. We note that the forces from the force plate are acting in the opposite direction since we calculated the the newton-euler forces in in a top-to-bottom way.
- The scaling errors seen in the Newton-Euler calculated the forces is probably due to discrepancy between the model and the real human body seen the complexity of the human articulation which can hardly be geometrically modeled and Numerical derivation errors due to the truncation of the higher order derivatives during the Taylor series expansion.
- We propose that this methodology can be used to closely represent the human motion as we see from the above plot that the forces are bounded and closely resemble those measured on the force plate, therefore can be reproduced on a robotics system, we can also see from the attached video files that the motion of the actor is closely reproduced in software.

The outcomes of the lab are as follows:

- Measurement of the segments of the actor
- Building the Modified Hanavan Model
- Capturing of human motions(Actor) and their analysis
- Simulation of Newton-Euler equations to compute forces and moments of the actor
- Model is finally validated using simulation results.
- Video Animation of the captured motion is also obtained